

**STUDIES OF SOME 3, 4-DICHLOROPHENACYL
ESTERS DERIVATIVES: SYNTHESIS,
CHARACTERIZATION, CRYSTAL STRUCTURE
DETERMINATION AND ANTIOXIDANT
PROPERTIES**

SIM AI JIA

UNIVERSITI SAINS MALAYSIA

2021

**STUDIES OF SOME 3, 4-DICHLOROPHENACYL
ESTERS DERIVATIVES: SYNTHESIS,
CHARACTERIZATION, CRYSTAL STRUCTURE
DETERMINATION AND ANTIOXIDANT
PROPERTIES**

By

SIM AI JIA

**Thesis submitted in fulfilment of the requirement
for the degree of
Master of Science**

March 2021

ACKNOWLEDGEMENT

I cannot express enough my gratitude to my principal supervisors, Assoc. Prof. Dr. Quah Ching Kheng and my co-supervisor, Dr. Suhana Arshad guided me through the whole process of learning by their superb in X-ray structure analysis and timely advice. My completion of this project which including the biological activity tests which have been accomplished in Taylor's University would give my sincere thanks to my field supervisor, Dr Mah Siau Hui and her master research fellows for their kindness in sharing knowledge and helps. Special thanks to the lab assistants and laboratory mates whom I met in School of Physics, Universiti Sains Malaysia by providing skills in running specific machine or equipment also valuable suggestions in writing a good thesis or reference papers. In addition, I would like to thanks Ministry of Higher Education Malaysia for giving me such an opportunity to get financial support in my education under MyBrain 15 scholarship. Finally, I am deeply thankful to my parent for their encouragement and supporting spirits always with me when the times got rough are much appreciated.

TABLE OF CONTENTS

ACKNOWLEDGEMENT.....	ii
TABLE OF CONTENTS.....	iii
LIST OF TABLES.....	vii
LIST OF FIGURES.....	viii
LIST OF ABBREVIATIONS.....	xiv
LIST OF APPENDICES.....	xv
ABSTRAK.....	xvi
ABSTRACT.....	xviii
CHAPTER 1 INTRODUCTION	
1.1 Background of Phenacyl Benzoates.....	1
1.2 Structure Identification.....	2
1.3 Problem Statement.....	3
1.4 Research Objectives.....	4
CHAPTER 2 LITERATURE REVIEW	
2.1 Literature Review on Phenacyl Benzoate Derivatives.....	5
2.2 Spectroscopy Studies.....	8
CHAPTER 3 EXPERIMENTAL TECHNIQUES AND INSTRUMENTATION	
3.1 Sample Preparation.....	12
3.2 Spectroscopic Instrumentation.....	13
3.2.1 Fourier Transform Infrared Spectroscopy (FT-IR).....	13
3.2.2 Nuclear Magnetic Resonance (NMR).....	14
3.3 Spectroscopic Studies.....	14
3.4 X-ray Crystallography Analysis.....	26

3.4.1	Software	26
3.4.1(a)	APEX2 Suite.....	26
3.4.1(b)	SHELXTL Software Package	27
3.5	Single Crystal X-ray Data Collection.....	30
3.5.1	Selecting Crystal	30
3.5.2	Data Collection and Processing	32
3.6	Structure Solution and Refinement	32
3.7	Hirshfeld Surface Analysis.....	36
3.8	Bioassays - Antioxidant Activity	38
3.8.1	Spectrophotometric Determination of Antioxidant Activity	38
3.8.2	2,2'-Diphenyl-1-picrylhydrazyl (DPPH) Radical Scavenging Assay.....	39
3.8.3	Ferrous Ion Chelating (FIC) Assay	40
3.8.4	Hydrogen Peroxide (H ₂ O ₂) Assay.....	40
3.9	Melting Point.....	41
CHAPTER 4 RESULTS AND DISCUSSIONS		
4.1	Introduction	42
4.2	3,4-Dichlorophenyl Benzoates Derivatives (Compounds 2a and 2r)	51
4.2.1	Data Collection and Structure Refinement	51
4.2.2	Crystal Structure Description.....	51
4.2.3	Crystal packing and Hirshfeld Surface Analysis	52
4.3	3,4-Dichlorophenyl Benzoates Derivatives (Compounds 2b-2e)	60
4.3.1	Data Collection and Structure Refinement	60
4.3.2	Crystal Structure Description.....	60
4.3.3	Crystal packing and Hirshfeld Surface Analysis	61

4.4	3,4-Dichlorophenyl Benzoates Derivatives (Compounds 2f , 2g and 2h) ...	68
4.4.1	Data Collection and Structure Refinement	68
4.4.2	Crystal Structure Description.....	69
4.4.3	Crystal packing and Hirshfeld Surface Analysis	70
4.5	3,4-Dichlorophenyl Benzoates Derivatives (Compounds 2i , 2j and 2k)	77
4.5.1	Data Collection and Structure Refinement	77
4.5.2	Crystal Structure Description.....	78
4.5.3	Crystal packing and Hirshfeld Surface Analysis	79
4.6	3,4-Dichlorophenyl Benzoates Derivatives (Compounds 2l , 2m and 2n)...	84
4.6.1	Data Collection and Structure Refinement	84
4.6.2	Crystal Structure Description.....	85
4.6.3	Crystal packing and Hirshfeld Surface Analysis	86
4.7	3,4-Dichlorophenyl Benzoates Derivatives (Compounds 2p and 2q).....	92
4.7.1	Data Collection and Structure Refinement	92
4.7.2	Crystal Structure Description.....	93
4.7.3	Crystal packing and Hirshfeld Surface Analysis	93
4.8	Spectroscopy Analysis of Benzoates Derivatives (2a-2s) (FT-IR, ¹ H-NMR and ¹³ C-NMR).....	100
4.9	Biological of Antioxidant Properties in Benzoates Derivatives (2a-2s) ..	106
CHAPTER 5 CONCLUSION AND FURTHER RECOMMENDATIONS		
5.1	Conclusion.....	111
5.2	Further Studies	112
REFERENCES.....		113
APPENDICES		
LIST OF PUBLICATIONS		

LIST OF TABLES

	Page
Table 3.1 General absences of bravais lattice type.....	33
Table 3.2 Systematic absences of 2_1 screw axes.....	33
Table 3.3 Systematic absences for glide planes.....	34
Table 4.1 Crystal data and parameters for structure refinement for 2(a-r) , except 2o).....	43
Table 4.2 Summary of the torsion angles τ_1 , τ_2 and τ_3 and dihedral 1 for 2(a-r) except 2o).....	46
Table 4.3 Hydrogen bond geometries for phenacyl benzoate derivatives 2(a-r) except 2o).....	48
Table 4.4 The FT-IR bond values for compound 2a-2s	102
Table 4.5 Antioxidant properties (DPPH and FIC) of compounds 2(a-s)	108
Table 4.6 Antioxidant properties (H_2O_2) of compounds 2(a-s)	109
Table 4.7 IC_{50} value of each compound for H_2O_2 radical scavenging Assay.....	110

LIST OF FIGURES

		Page
Figure 1.1	Chemical structure of benzoate structure.....	1
Figure 2.1	Chemical structure of phenacyl bromide.....	5
Figure 2.2	Crystal packing of amino-substitution of benzoate compounds (Chidan Kumar <i>et al.</i> , 2014).....	7
Figure 2.3	(a) Scheme and (b) the crystal packing of the molecular structures of 2-(Benzofuran-2-yl)-2-oxoethyl 4-nitrobenzoates (Chidan Kumar <i>et al.</i> , 2015).....	8
Figure 2.4	(a) Molecular view of the compound and (b) the crystal packing of the molecular structures of 2-(Benzofuran-2-yl)-2-oxoethyl 4-nitrobenzoates (Chidan Kumar <i>et al.</i> , 2014).....	9
Figure 2.5	FTIR, ¹ H and ¹³ CNMR spectra of 2-(adamantan-1-yl)-2-oxoethyl benzoates (Chidan Kumar <i>et al.</i> , 2015).....	11
Figure 3.1	Reaction scheme for 2(a-s)	13
Figure 3.2	The APEX2 software diagram (<i>APEX2 User Manual Version 2</i> , 2006).....	27
Figure 3.3	The schematic diagram showing the process of structure determination using SHELXTL programs.....	28
Figure 3.4	Crystals formed in a beaker (viewed under light microscope).....	30
Figure 3.5	A crystal mounted on a copper pin (viewed from video microscope).....	31
Figure 3.6	Examples of (a) a strongly reflecting sample (crystalline) and (b) a weakly reflecting sample (amorphous).....	31
Figure 3.7	The distance d_e and d_i are illustrated schematically between the Hirshfeld surface of the molecule which is shown in grey region and the nearest molecule surface at the red point (Spackman & McKinnon, 2002).....	37
Figure 3.8	Biotek Epoch 2 Microplate Reader.....	38

Figure 3.9	Genesys™ 10S UV-Vis Spectrophotometer.....	39
Figure 4.1	General chemical scheme for all compounds, showing τ_1 , τ_2 , and τ_3 as torsion angles.....	46
Figure 4.2	<i>ORTEP</i> diagram of compound 2a and 2r with 40% ellipsoid probability and their atomic labelling scheme.....	51
Figure 4.3	Hydrogen bonds in 2a links the molecules into chains along <i>a</i> -axis.....	53
Figure 4.4	Intermolecular C—H···O hydrogen bonds (cyan dotted lines) form dimeric structures in compound 2a	53
Figure 4.5	Packing of 2a involving C—H···O hydrogen bonds shown in cyan dashed line, dimers shown in magenta dashed line and C—H···Cl hydrogen bonds shown in yellow dashed line.....	54
Figure 4.6	Packing diagram of 2r , blue dotted lines indicate the π ··· π interactions formed between two chains and magenta dotted lines indicates the C—H··· π interactions.....	54
Figure 4.7	The ball and stick models, d_{norm} and electrostatic potential mapped on Hirshfeld surface for visualizing the intermolecular contacts in compounds 2a (molecules <i>A</i> and <i>B</i>) and 2r	57
Figure 4.8	d_{norm} and electrostatic potential mapped on Hirshfeld surfaces of compound 2a and 2r used to visualize the C—H···O and C—H···Cl hydrogen bonds. Hydrogen bonds are represented by dashed lines.....	58
Figure 4.9	Hirshfeld surfaces of compound 2r mapped over (a) shape index and (b) the curvedness.....	58
Figure 4.10	Fingerprint plots for compounds 2a-A (molecule <i>A</i>), 2a-B (molecule <i>B</i>) and 2r , respectively. The grey shadow for each plot is an outline of the complete fingerprint plot.....	59
Figure 4.11	<i>ORTEP</i> diagram of molecular compounds 2b–2e was drawn at 40% ellipsoid probability with atomic labelling scheme.....	60
Figure 4.12	(a) Crystal packing diagram of 2b with molecule <i>A</i> and molecule <i>B</i> interconnected into 2D corrugated sheets.....	62
Figure 4.13	Compound 2c shows the inversion related dimers propagating along <i>b</i> -axis in crystal packing.....	63

Figure 4.14	Partial crystal packing of 2d , showing C—H··· π interaction molecules.....	63
Figure 4.15	Partial packing of 2e , bifurcated C—H···O hydrogen bonds join adjacent molecules into <i>zigzag</i> chain.....	63
Figure 4.16	The ball and stick models, d_{norm} and electrostatic potential mapped on Hirshfeld surface for visualizing the intermolecular contacts in compounds 2b–2e	65
Figure 4.17	Fingerprint plots for 2b-A (molecule A), 2b-B (molecule B), 2c , 2d and 2e compounds, respectively. The grey shadow for each plot is an outline of the complete fingerprint plot.....	66
Figure 4.18	d_{norm} and electrostatic potential mapped on Hirshfeld surfaces of compound 2b , 2c and 2e for visualizing the C—H···O interactions.....	67
Figure 4.19	(i) d_{norm} , (ii) electrostatic potential, (iii) shape index and (iv) curvedness mapped on Hirshfeld surfaces of compound 2d to visualize the weak intermolecular C—H··· π interactions.....	68
Figure 4.20	Molecular structure with 40% ellipsoid probability and atomic labelling scheme in compounds 2f–2h	69
Figure 4.21	Partial packing diagram of 2f	71
Figure 4.22	Partial packing diagram of compound 2g , showing inversion related dimer chain.....	71
Figure 4.23	Partial packing diagram of 2h with chained molecule A and molecule B. (b) Partial packing diagram of 2h with chained molecule C.....	72
Figure 4.24	Packing diagram of 2h with intra-chain hydrogen bonds shown in cyan dashed line and inter-chain hydrogen bonds shown in magenta dashed line.....	72
Figure 4.25	(i) d_{norm} , (ii) electrostatic potential, (iii) shape index and (iv) curvedness mapped on Hirshfeld surfaces of compound 2f to visualize the weak intermolecular C—H···O and C—H··· π interactions.....	74
Figure 4.26	d_{norm} and electrostatic potential mapped on Hirshfeld surfaces for visualizing the intermolecular C—H···O interactions of the 2g and 2h compounds.....	75

Figure 4.27	The ball and stick models, d_{norm} and electrostatic potential mapped on Hirshfeld surface for visualizing the intermolecular contacts in compounds 2f , 2g and 2h (molecules <i>A</i> , <i>B</i> and <i>C</i>).....	76
Figure 4.28	Fingerprint plots for 2f , 2g , 2h-A (molecule <i>A</i>), 2h-B (molecule <i>B</i>) and 2h-C (molecule <i>C</i>) compounds, respectively, classified into contributions with specific close contacts.....	77
Figure 4.29	Compounds 2i-2k were drawn at 40% ellipsoid probability with suitable atomic labelling and are shown in <i>ORTEP</i> diagram.....	78
Figure 4.30	Partial packing diagram of 2i	80
Figure 4.31	(a) Partial packing diagram of compound 2j , showing hydrogen bonded dimer chain (cyan dashed lines). (b) Partial packing of compound 2j with Cl···Cl short contact (green dashed lines).....	80
Figure 4.32	Packing diagram of compound 2k , (a) showed central symmetry dimers. (b) showed the two dimensional plate parallel to <i>a,b</i> -plane.....	81
Figure 4.33	The ball and stick models, d_{norm} and electrostatic potential mapped on Hirshfeld surface for visualizing the intermolecular contacts in compounds 2i , 2j and 2k (molecules <i>A</i> and <i>B</i>).....	82
Figure 4.34	The 2-dimensional fingerprint plot for the 2i-2k compounds showing contributions from different d_{norm} surface associated with the specific H···H, O···H/H···O C···H/H···C, and Cl···H/H···Cl contacts.....	83
Figure 4.35	Views of Hirshfeld surface of 2i-2k compounds mapped over d_{norm} for the atoms O1A, O3A, H4A, H8A, H8B and H5B near to red spots on the surfaces.....	84
Figure 4.36	Molecular structure of 2l-2n with 40% ellipsoid probability with atomic labelling ARE shown in <i>ORTEP</i> style.....	85
Figure 4.37	Packing diagram of 2l with intra-chain hydrogen bonds shown in cyan and yellow dashed line and inter-chain hydrogen bonds shown in magenta dashed line.....	86
Figure 4.38	Partial packing of 2m , molecules are linked along <i>b</i> -axis via C—H···O hydrogen bonds.....	87

Figure 4.39	Partial packing diagram of compound 2m , showing C5—H5A···O4 hydrogen bonds (magenta dashed line) are interconnected with dimer chains into sheets parallel to <i>b</i> , <i>c</i> -plane.....	87
Figure 4.40	C—H···O hydrogen-bonds linked the two adjacent Molecules A and molecule B in 2n into sheets parallel to <i>a</i> , <i>b</i> -plane.....	88
Figure 4.41	Crystal packing of 2n , showing the abundant interactions that involved nitro groups.....	89
Figure 4.42	The ball and stick models, d_{norm} and electrostatic potential mapped on Hirshfeld surface for visualizing the intermolecular contacts in compounds 2l , 2m and 2n (molecules A and B).....	90
Figure 4.43	The 2-dimensional fingerprint plot for the 2l–2n compounds showing contributions from different d_{norm} surface associated with the specific H···H, O···H/H···O C···H/H···C, and Cl···H/H···Cl contacts.....	91
Figure 4.44	Visualization of intermolecular C—H···O interactions between molecules in compounds 2l–2n through d_{norm} and electrostatic potential mapped on Hirshfeld surfaces.....	92
Figure 4.45	Compound 2p and 2q were drawn at 40% ellipsoid probability with atomic labelling scheme.....	93
Figure 4.46	Partial packing of 2p , viewed along <i>b</i> -axis.....	94
Figure 4.47	Extensive interactions in compound 2p , viewed along (a) <i>a</i> - and (b) <i>b</i> -axes.....	94
Figure 4.48	(a) N—H···O and C—H···O hydrogen bonds link the molecules of 2q into a 1D assembly. (b) Partial packing of 2q showing inversion related dimers.....	95
Figure 4.49	The packing pattern of compound 2q showing 2D corrugated sheets.....	96
Figure 4.50	The ball and stick models, d_{norm} and electrostatic potential mapped on Hirshfeld surface for visualizing the intermolecular contacts in compounds 2p and 2q	97
Figure 4.51	The 2-dimensional fingerprint plot for the 2p and 2q compounds showing contributions from different d_{norm} surface associated with the specific H···H, O···H/H···O C···H/H···C, and Cl···H/H···Cl and N···H/H···N contacts.....	98

Figure 4.52	d_{norm} and electrostatic potential mapped on Hirshfeld surface for visualizing the hydrogen bonds in compounds 2p and 2q	99
Figure 4.53	(i) d_{norm} , (ii) electrostatic potential (iii) shape index (iv) curvedness mapped on Hirshfeld surface for visualizing the C—H··· π interactions in compounds 2p	99
Figure 4.54	FTIR spectrum for 2-(3, 4-dichlorophenyl)-2-oxoethyl nicolinate (2s).....	104
Figure 4.55	¹³ C-NMR spectrum for 2-(3, 4-dichlorophenyl)-2-oxoethyl nicolinate (2s).....	105
Figure 4.56	¹ H NMR spectrum for 2-(3, 4-dichlorophenyl)-2-oxoethyl nicolinate (2s).....	106
Figure 4.57	H ₂ O ₂ radical scavenging assay. The data represent the concentration at 50% radical inhibition of compounds, and experiments were carried out in triplicate.....	110

LIST OF ABBREVIATIONS

3D	Three-dimensional
a, b, c, α , β , γ	Unit-cell parameters
IUPAC	International Union of Pure and Applied Chemistry
CSD	Cambridge Structural Database
wR	Weighted Reliability Index
R	Reliability Index
<i>Goof/S</i>	Goodness of fit
FT-IR	Fourier Transform Infrared
NMR	Nuclear Magnetic Resonance
DPPH	Diphenyl-2-picrylhydrazyl
FIC	Ferrous Ion Chelating
H ₂ O ₂	Hydrogen peroxide
ATR	Attenuated total reflection
SMART	Siemens Molecular Analysis Research Tools
CCD	Charge-Coupled Device
BIS	Bruker Instrument Service
GUI	Graphical User Interface
ORTEP	Oak Ridge Thermal Ellipsoid Plot
TLC	Thin-layer chromatography
IC ₅₀	Half maximal inhibitory concentration
$\mu\text{g/ml}$	Microgram per Millilitre
$^{\circ}\text{C}$	Degree Celsius
ν	Wavenumber

ν	Stretching
δ	Chemical Shift/Bending
^1H	Proton
^{13}C	Carbon-13
s	singlet
d	doublet
t	triplet
m	multiplet
TLC	Thin Layer Chromatography
DMF	Dimethylformamide
SADABS	Siemens Area Detector Absorption Correction
SAINT	SAX Area-detector Integration (SAX-Siemens Analytical X-ray)
SD	Standard Deviation
τ	Torsion Angle
Z'	Asymmetric Unit
vdW	Van der Waals

LIST OF APPENDICES

APPENDIX A BOND LENGTHS OF THE TITLE COMPOUNDS

APPENDIX B ^1H NMR, ^{13}C NMR AND FT-IR SPECTRUM

**KAJIAN BEBERAPA TERBITAN 3, 4-DIKLOROFENIL ESTERS: SINTESIS,
PENCIRIAN, PENENTUAN STRUKTUR HABLUR DAN SIFAT
ANTIOKSIDA**

ABSTRAK

Dalam kajian ini, satu siri sembilan belas 3, 4-diklorofenil esters **2(a-s)** telah disintesis dan dihaburkan melalui penyejatan secara perlahan. Semua struktur hablur telah dicirikan dengan analisi spektroskopi FTIR dan NMR dan seterusnya ditentukan dengan kristalogafi pembelauan sinar-X hablur tunggal kecuali **2o** and **2s**. Konformasi molekular dan padatan hablur bagi sebatian ini telah dianalisis dengan kaedah kristalografi. Lapan sebatian telah terhablur dalam kumpulan ruang monoklinik $P2_1/c$ atau $P2_1/n$, tujuh dalam triklinik $P\bar{1}$, manakala dua dalam ortorombik $Pna2_1$ atau $Pbca$. Dalam sebatian ini, gelang 3, 4-diklorofenil telah disambung dengan titian penyambung $C(=O)-O-C-C(=O)$ dan menyambungkannya dengan pelbagai gelang fenil planar bergantian. Sebahagian titian penyambung berada dalam konformasi klinal antara dua kumpulan karbonil, manakala konformasi antara karbonil dan setiap fenil adalah hampir mendatar ataupun sedikit berpintal disebabkan kesan tolakan sterik mereka dalam setiap bahagian. Dalam padatan hablur, ikatan hidrogen $C-H \cdots O$ (konvensional) terlibat dalam semua sebatian kecuali sebatian **2d** yang cuma melibatkan interaksi $C-H \cdots \pi$ (bukan konvensional). Aktiviti antioksidasi bagi semua sebatian yang baru disintesis telah dinilai dengan ujian 2, 2-difenil-1-picrylhydrazyl (DPPH), chelator besi oral (FIC) and hidrogen peroksida (H_2O_2). Kesan perencatan radikal dari terbitan fenacil adalah berkait dengan kumpulan penderma electron dan penerima bagi

penganti pada gelang fenil yang bersangkutan. Sebatian **2s**, **2p**, **2j**, **2h** dan **2b** menunjukkan potensi kesan perencatan dalam kajian H_2O_2 radikal.

**STUDIES OF SOME 3, 4-DICHLOROPHENACYL ESTERS DERIVATIVES:
SYNTHESIS, CHARACTERIZATION, CRYSTAL STRUCTURE
DETERMINATION AND ANTIOXIDANT PROPERTIES**

ABSTRACT

In this research, a series of nineteen 3, 4-dichlorophenacyl esters **2(a-s)** were synthesized and crystallized by using slow evaporation method. The crystal structures were characterized by FT-IR and NMR spectroscopic analyses and further determined by single crystal X-ray crystallography technique (except **2o** and **2s**). The molecular conformation and crystal packing of these compounds were studied crystallographically. Eight compounds crystallized in monoclinic $P2_1/c$ or $P2_1/n$ space group, seven in triclinic $P\bar{1}$, whereas two in orthorhombic $Pna2_1$ and $Pbca$. In these compounds, the planar 3, 4-dichlorophenyl ring is connected by C(=O)—O—C—C(=O) connecting bridge to various planar substituted phenyl ring. Most of the connecting bridges adopted *clinal* conformation between two carbonyl groups, while the conformations between carbonyl and each phenyl rings are nearly planar or slightly twisted due to their steric repulsion effect within each moiety. In the crystal packing, C—H \cdots O hydrogen bonds (conventional) are involved in all of the compounds except compound **2d** which is only involved C—H \cdots π interactions (non-conventional). The antioxidant activities of all newly synthesized compounds were assessed using 2, 2-diphenyl-1-picrylhydrazyl (DPPH), ferrous ion chelating (FIC) and hydrogen peroxide (H₂O₂) radical scavenging assays. Radical inhibition effects of phenacyl derivatives are related to the electron donating and accepting groups of the substituents

at their attached benzene rings. Compounds **2s**, **2p**, **2j**, **2h** and **2b** showed potential inhibitory effect towards the H₂O₂ radical scavenging assay.

CHAPTER 1

INTRODUCTION

1.1 Background of Phenacyl Benzoates

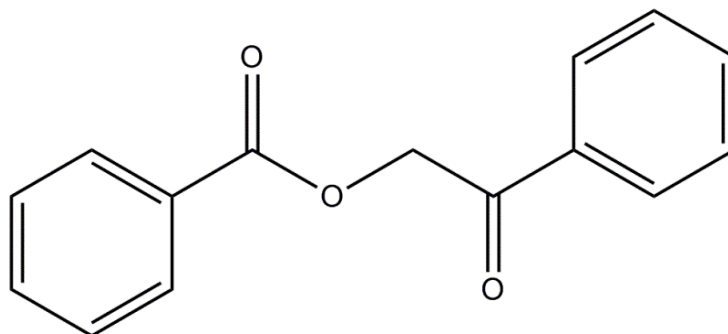


Figure 1.1 Chemical structure of benzoate structure.

Phenacyl benzoates (Figure 1.1) is an organic compound that contains functional groups of a ketone and an ester with the general molecular formula $C_{15}H_{12}O_3$. They are synthesized from the reaction of phenacyl bromide with benzoic acid. Organic acids or ester derivatives are useful for identification purposes and playing vital role as protecting groups for carboxylic acids in organic synthesis and chemistry since photoremovable protecting groups provide spatial and temporary control over the release of various chemical such as bioagents, acid, bases and *etc* (Ruzicka *et al.*, 2002). These are also the photosensitive blocking groups with the ease of cleaving under mild conditions and therefore used for the identification of organic acids. Phenacyl benzoates's growing research interests is attributable to their biological activities. which have been reported possessing significant antitumor activities against Ehrlich cells and HeLa cells (Diwaker *et al.*, 2015). These noteworthy potentials are frequently used in organic synthesis and they act as key intermediates or starting materials used in the preparation of more stable derivatives keto esters, mercaptals, pyrazoles and enamines (Pal *et al.*, 2008), (Stanovnik & Svete, 2004) and (Hassan *et al.*, 2006).

1.2 Structural Identification

X-ray crystallography has been introduced to discover the atomic and molecular structure of a crystal which the X-rays were first discovered and studied by a German physicist, William Conrad Röntgen in 1895. The properties of X-ray diffraction and Bragg's Law have given great contributions in this technique by later scientists (Schneegans, 2014) and (*Bragg & William Lawrence*, 2009) to explore and give further information on the internal structure of a crystal. Nuclear magnetic resonance spectroscopy (NMR), gas chromatography–mass spectrometry (GCMS), Raman spectroscopy and Fourier-transform infrared spectroscopy (FT-IR) are among some of the modern instrumental techniques used for structural elucidation. Single-crystal X-ray diffraction method provides more details on the three-dimensional (3D) model of molecular structure with the types and mean position of atoms in the crystal are determined and assigned precisely unambiguously if compared to previous conventional methods. From the X-ray diffraction analysis, electron density map can be calculated to reveal the conformational and geometrical parameters in crystal structure. In addition, intermolecular interaction studies reveal the chemical, physical, mechanical and electrical properties of a crystalline material. For a supramolecular structure, besides strong intermolecular interactions such as hydrogen bonding, it also involves many weaker other non-covalent interactions such as van der Waals, hydrophobic interactions, short contacts and C—H \cdots π / π \cdots π interactions in which these interactions rely on the nature of the chemical building blocks in the molecules. Supramolecular complexes bearing different functional groups (or chemical moieties) will result in different packing coefficients due to the impact of various intermolecular forces. These crystal packings and their conformations may provide extra information for the synthesis of novel molecular structures or in

structural modification in pharmaceutical fields. Single-crystal X-ray technique provides clear visualization of the molecular structures and their supramolecular networks. Hirshfeld surfaces analysis has been studied to identify and analyse all close contacts and different types of intermolecular interactions within crystal structures. This technique is very useful in studying the effects of different functionalities towards the crystal packing behaviour. Nevertheless, obtaining a good crystalline material is one of the toughest limitations in employing the X-ray diffraction method and there are many methods of crystallization process which are not an ease (Deschamps, 2010). As time goes by, X-ray crystallography technique has been improved constantly through the advancement of computational power, sensitivity of X-ray detector and power of the X-rays generated. Nowadays, unknown compounds obtained from natural products and synthetic processes can be identified using X-ray crystallography method and contributes to pharmacology, mineralogy, biochemistry and materials science fields.

1.3 Problem Statement

The excessive of free radicals in human cell which may lead to malfunction of organs or even cause dead. This issue has attracted many researchers' attentions to invest the best antioxidant agent to reduce the risk of excessive free radicals which may cause harmful to human body. In recent years, phenacyl esters are highlighted by the researcher which act as good antioxidant agents especially in pharmaceutical industries. The properties of antioxidant is depending on the physical properties of the phenacyl ester. In other words, the arrangement of molecules in crystal packing will directly impact to the polymorphism of the drugs design. Thus, the derivatives of benzoic acids with different functional groups must be identified, synthesized and characterized for their structural properties which their potential antioxidant properties

could be discovered. Besides, Single Crystal X-ray Diffraction was introduced to identify the crystal structures with three-dimensional network and the supramolecular structures which give a platform for structure-based drug design in rapid testing of biological activities purpose.

In this project research, nineteen newly modified phenacyl benzoates derivatives are synthesized with different functional groups to identify the best antioxidant agent to inhibit the free radicals in human body (Then *et al.*, 2018).

1.4 Research Objectives

The three main aims of this research projects are:

- i. To synthesize a series of phenacyl benzoates derivatives and to characterize their structures using NMR and FT-IR spectroscopy.
- ii. To study the crystal structure and supramolecular construct of newly synthesized compounds by using single crystal X-ray diffraction technique and Hirshfeld surface analysis.
- iii. To evaluate the antioxidant inhibitory activities of title compounds.

CHAPTER 2

Literature Review

2.1 Literature Review on Phenacyl Benzoates Derivatives

Phenacyl benzoates attract commercial importance due to their various applications in the field of synthetic and photo-chemistry. Apart from that, phenacyl bromide has an advantage and easily be prepared if compared to its counterpart, phenacyl chloride, which gives lower yields of benzoate derivatives (Rather & Reid, 1919). Due to high reactivity of ketone moiety which attached to the bromobenzene ring, they react with the large number of nucleophiles which provide a range of biological active compounds. The reported bromoacetophenone derivatives have been examined for their active contribution in inhibition of protein tyrosine phosphatase bioactivities. The reactive sites of the ketone compounds would increase the bioactivity, mainly cytotoxicity against breast cancer cells (Vekariya *et al.*, 2017) and (Narender *et al.*, 2005). The crystal structure of phenacyl bromide was shown in Figure 2.1.

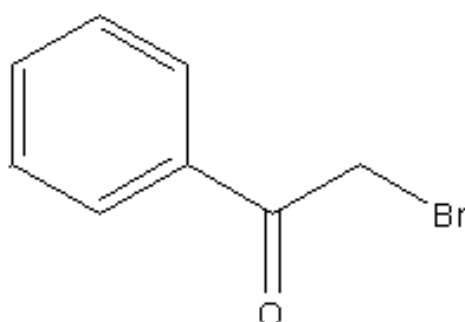


Figure 2.1 Chemical structure of phenacyl bromide.

The synthesized phenacyl benzoates also give significance results in antimicrobial activity against gram-positive and gram-negative bacteria and two fungal pathogenic strains, respectively (Khan *et al.*, 2018). The modification of

molecular structure on the basic skeleton with different substituent will affect the antimicrobial activity which is reported in review article (Khan *et al.*, 2016). Moreover, phenacyl benzoate derivatives could be designed as photosensitive blocking groups for amino and carboxyl function (peptide synthesis) in biochemistry aspect which give advantage of removing themselves completely under mild and neutral conditions (Sheehan & Umezawa, 1973). Apart from biological properties, benzoate derivatives also can be considered as a starting material for production of electrical components with high conductivity properties (McKean & Stille, 1987), and optical poling in fibre optics (Kityk *et al.*, 2004).

Chidan Kumar *et al.* (2014) have studied the structural behaviors of newly 2-bromophenyl-oxoethyl benzoates derivatives with various substituted benzoic acids and characterized by mass spectrometer and melting points. The 3D structure was confirmed by single crystal X-ray diffraction studies. The C(=O)—O—C—C(=O) connecting bridge between two phenyl rings was confirmed by the X-ray 3D structures with the torsion angles of 70 to 90°. In the crystal packing of these compounds (Figure 2.2), strong classical N_{amino}—H···O hydrogen bonds dominate in the crystal structures which relate to their higher melting points. Due to the significant strong hydrogen bonds form in the supramolecular interactions among the crystal structures, compounds with amino substituents showed better antioxidant properties (Chidan Kumar *et al.*, 2014). For instant, *p*-Aminobenzoic acid found in vitamin B group is one of the pharmaceutically relevant tiny organic molecules showed good free radical scavenging activity which has used as a prophylactic in cosmetics against skin

disorders by exposing to UV sunlight (Sowinska *et al.*, 2019).

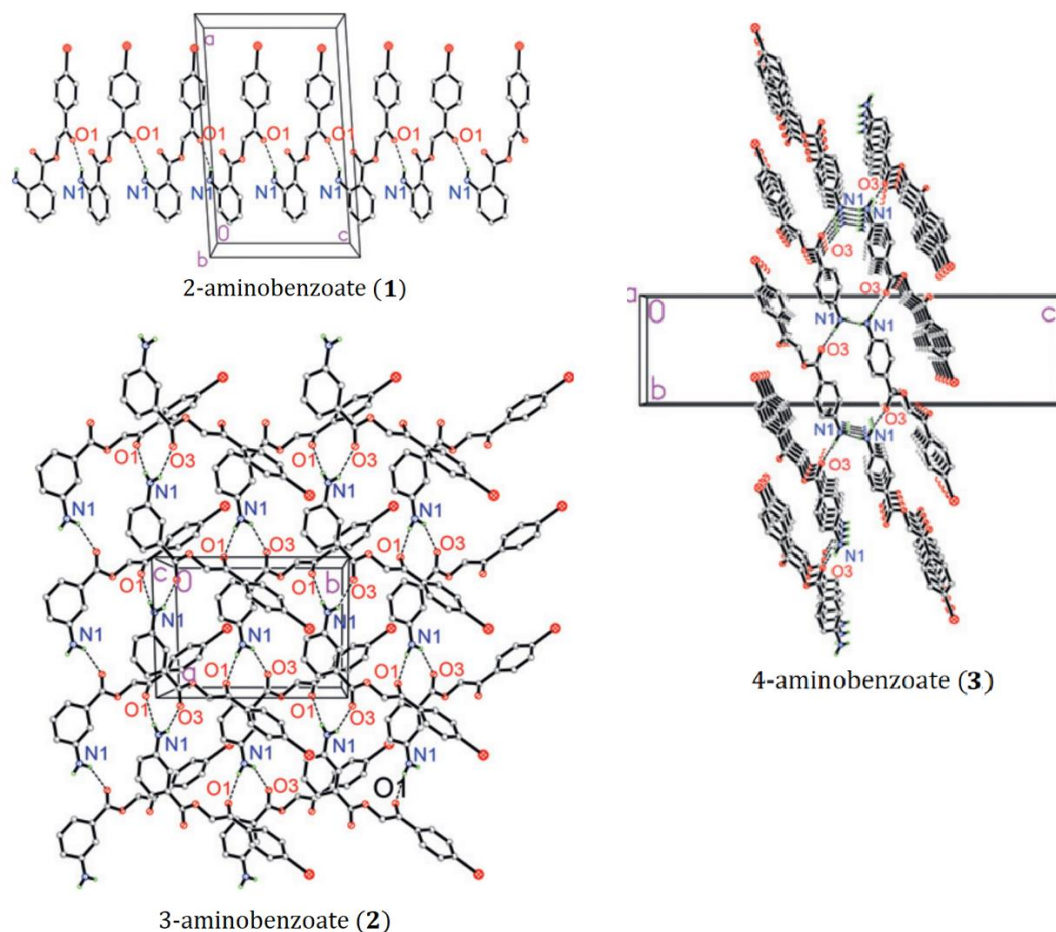


Figure 2.2 Crystal packing of amino-substitution of benzoate compounds (Chidan Kumar *et al.*, 2014).

The crystal structures of benzofuran with different functional groups of benzoic acids studied by Chidan Kumar *et al.* (2015) shows that nitro-substituted at phenyl ring compound give the better antimicrobial and antioxidant abilities which may be treated as a potential antimicrobial and antioxidant activities. The molecules in 2-(Benzofuran-2-yl)-2-oxoethyl 4-nitrobenzoates are linked by weak C—H...O hydrogen bonds and $\pi \cdots \pi$ interactions into a three-dimensional network (Figure 2.3). Due to the layered structure of $\pi \cdots \pi$ interactions in the crystal packing of compound, the stability of supramolecular structures may enhance the free radical scavenging inhibition in antioxidant activities.

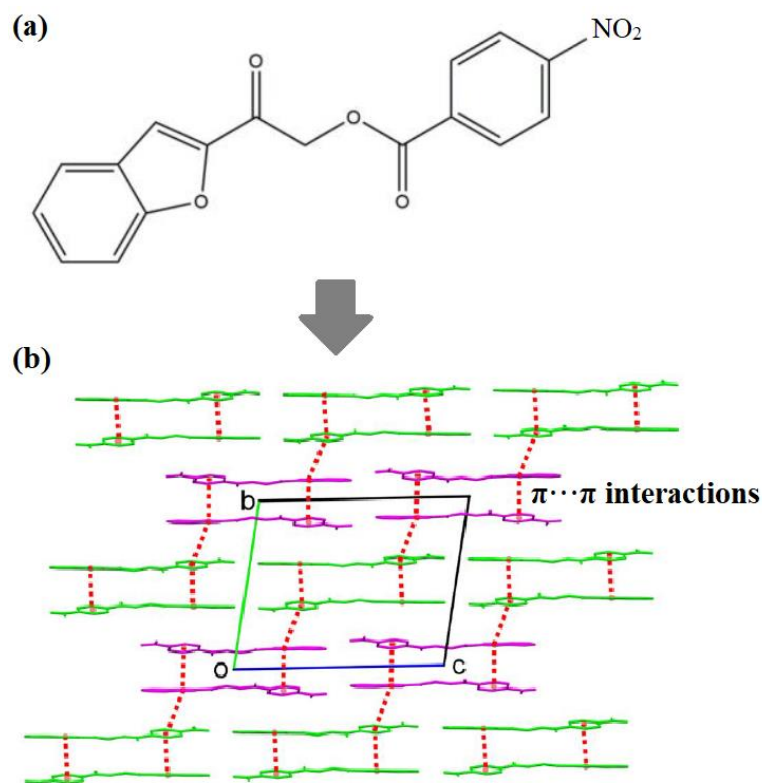


Figure 2.3 (a) Scheme and (b) the crystal packing of the molecular structures of 2-(Benzofuran-2-yl)-2-oxoethyl 4-nitrobenzoates (Chidan Kumar *et al.*, 2015).

2.2 Spectroscopic Studies

IR spectroscopy analysis for 2-(4-chlorophenyl)-2-oxoethyl 2-chlorobenzoate was discussed by Chidan Kumar *et al.* (2014). In their structures, the vibrational spectra for C–H and C–C modes of vibrations can be indicated in related aromatic compounds. In the benzene ring, frequencies of C–H stretching band are observed at higher wavenumber of 3097, 3079 and 3043 cm^{-1} which the predominant vibrations are affected by the smaller mass of the hydrogen atom attached to the carbon atom in aromatic ring. The vibrational interactions are also referring to one of the characteristics of intermolecular C–H \cdots O hydrogen bonds that links the molecules to form a 2D corrugated sheets in crystal packing. The C–H stretching bands are consistent occurring at the same frequency bands with previously reported chlorobenzoic acids (Lee & Li, 1996) and (Takashima *et al.*, 1999). The C–C

stretching bands are determined in the structures (1625 cm^{-1} – 1280 cm^{-1}) and the vibrations are within the expected range which can be considered not much affected by the position of the substituent around the ring. The C–Cl stretching modes are found in the lowest frequency region due to the greater mass of chlorine atom. Figure 2.4 shows the FTIR spectrum recorded in the range 400 cm^{-1} – 3400 cm^{-1} at room temperature.

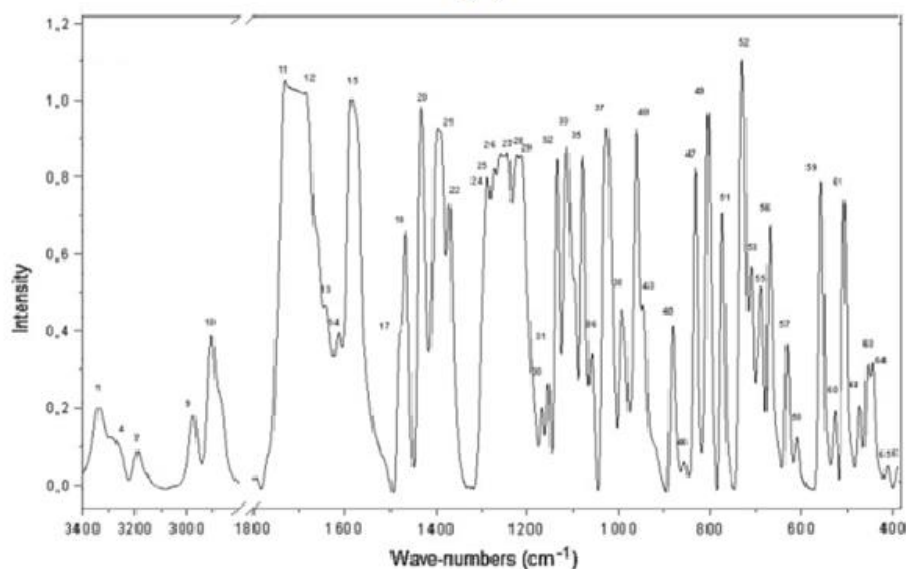
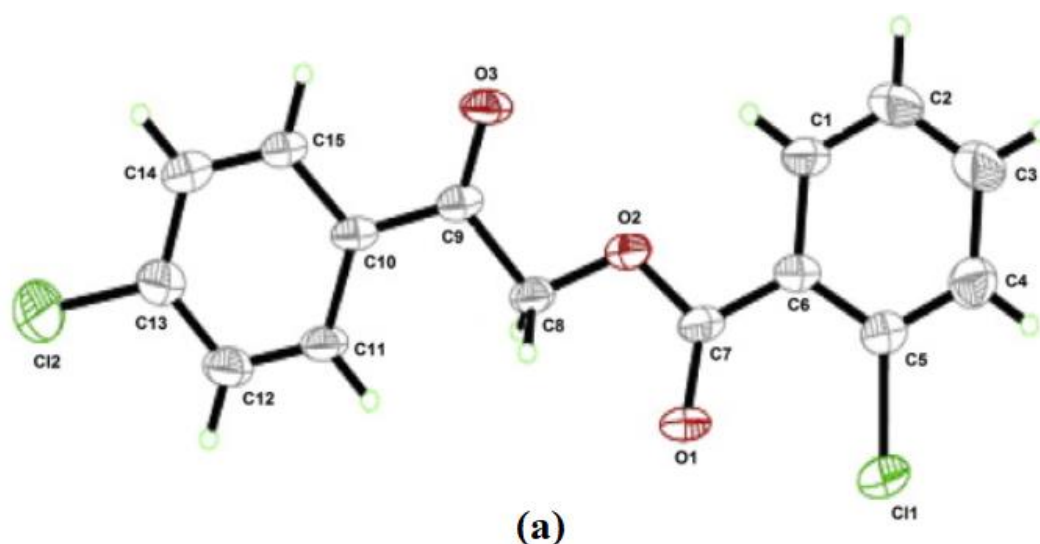


Figure 2.4 (a) Molecular view of the compound and (b) the crystal packing of the molecular structures of 2-(Benzofuran-2-yl)-2-oxoethyl 4-nitrobenzoates (Chidan Kumar *et al.*, 2014).

Chidan Kumar *et al.* (2015) has reported the IR and NMR spectrum of benzoate ester derivatives. In FTIR spectrum, the absorption bands of the unsaturated C–H (aromatic) groups are located above 3000 cm^{-1} . The N=O stretching, N–H stretching and C–N stretching are observed at the real positions in vibrations. In proton (^1H) NMR, the signals of the significant $-\text{CH}_2-$ protons in the connecting bridge are revealed as a singlet centered at $\delta \approx 5.10\text{ ppm}$. Protons near the methyl and methoxy groups attached to the benzene ring were found upfield, near $\delta \approx 2.50$ to 3.90 ppm , respectively. In the ^{13}C spectrum, the signals of the aromatic carbons are revealed at downfield region in the range of $\delta \approx 163$ – 110 ppm and $\delta \approx 66\text{ ppm}$ are assigned to the saturated carbon signal of methylene group ($-\text{CH}_2-$). Furthermore, both $\delta(\text{C}=\text{O})$ and $\delta(\text{COO})$ carbonyl signals are downfield, centered around $\delta \approx 207\text{ ppm}$ and 166 ppm . A representative FTIR, ^1H and ^{13}C NMR spectra of 2-(adamantan-1-yl)-2-oxoethyl benzoates are shown in Figure 2.5.

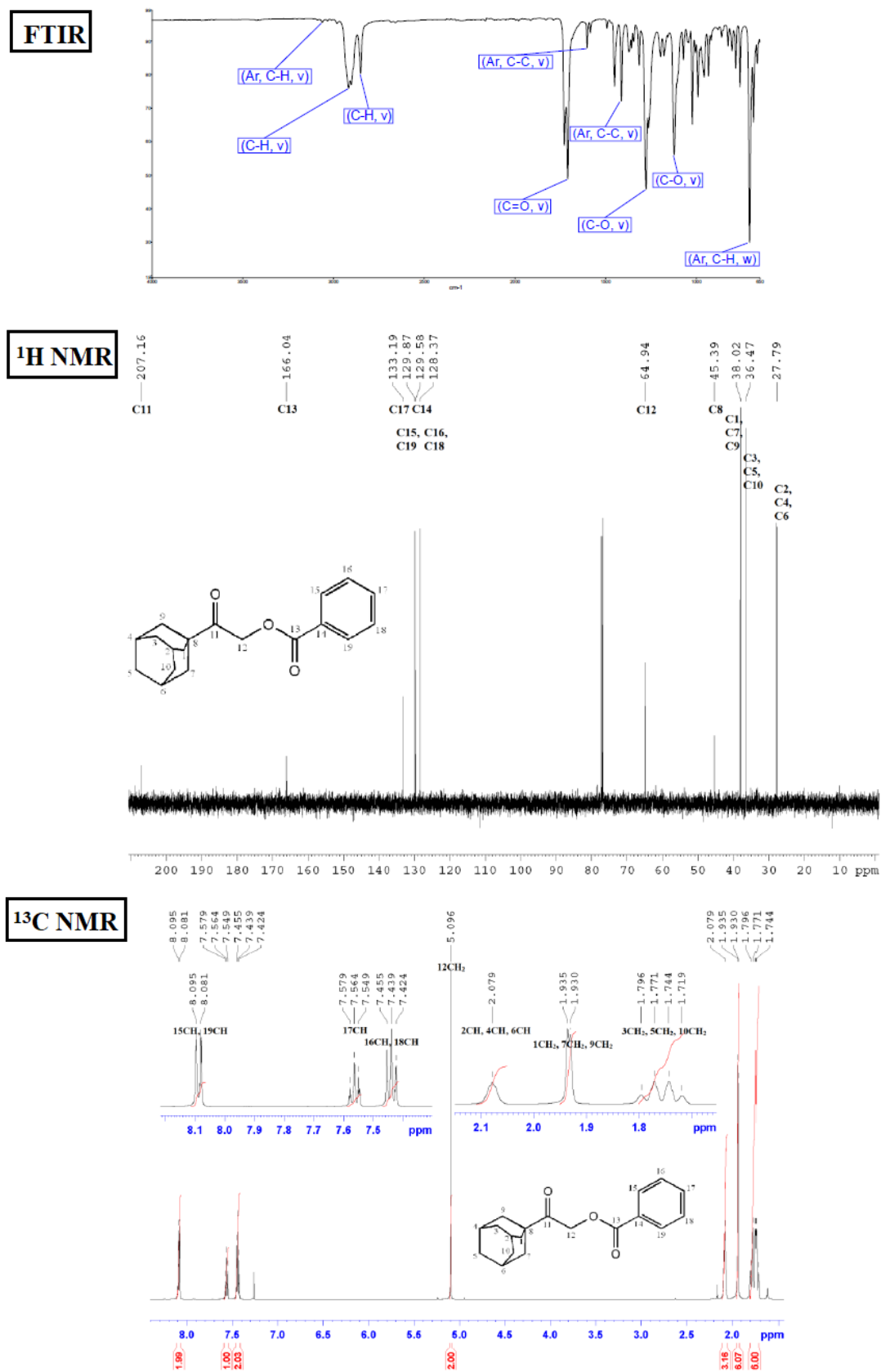


Figure 2.5 FTIR, ¹H and ¹³CNMR spectra of 2-(adamantan-1-yl)-2-oxoethyl benzoates (Chidan Kumar *et al.*, 2015).

CHAPTER 3

EXPERIMENTAL TECHNIQUES AND INSTRUMENTATION

3.1 Sample Preparation

Phenyl benzoates derivatives were synthesized by undergoing a two-step reaction (Figure 3.1). Firstly, 1-(3, 4-dichlorophenyl) ethanone was refluxed with *N*-bromosuccinimide and petroleum ether in methanol at 333 K for two hours. The resultant precipitate 2-bromo-1-(3, 4-dichlorophenyl) ethanone (**1**) was filtered and crystallized with ethanol. Next, 2-bromo-1-(3, 4-dichlorophenyl) ethanone (**1**) (0.3g, 0.001 mol) was reacted with the substituted benzoic derivatives (0.4g) in the presence of anhydrous potassium carbonate (0.003mol) in dimethylformamide (8 mL). The solution was stirred for 4 hours at room temperature. The progress of the reaction was monitored by thin-layer chromatography (TLC). The reaction mixture was poured into ice-cool water once the reaction was completed and kept stirring for 10 minutes. The precipitates obtained were then filtered, air dried and recrystallized by using appropriate solvent in order to receive good yield and high purity. Crystal structures of all compounds, except **2o** and **2s**, were determined by single-crystal X-ray diffraction analysis.

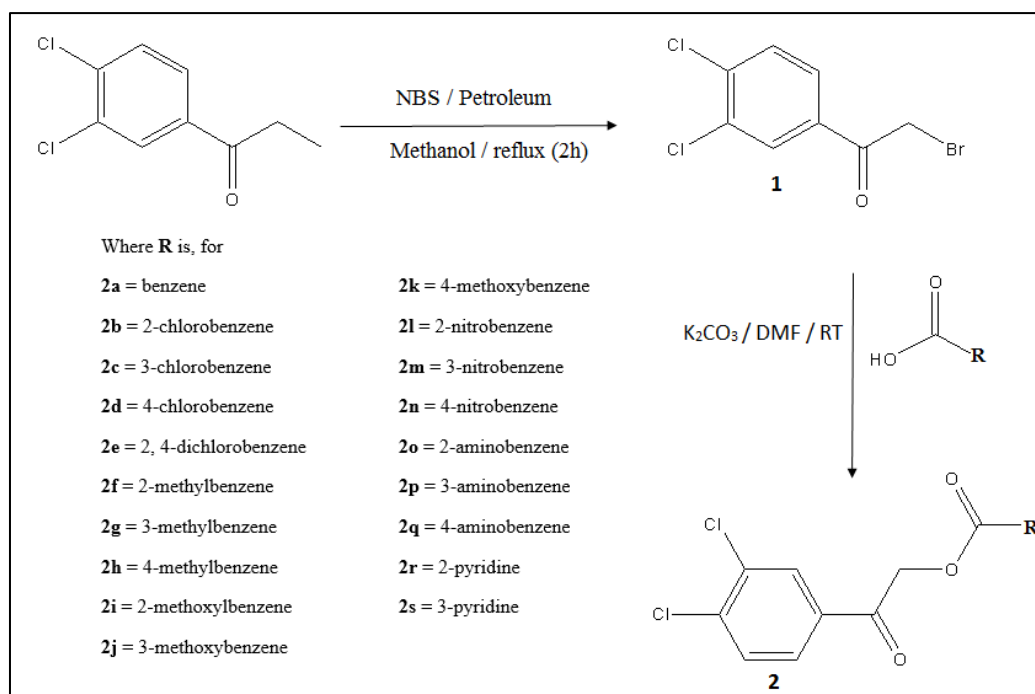


Figure 3.1 Reaction scheme for **2(a-s)**.

3.2 Spectroscopy Instrumentation

The grown crystals were characterized using two different spectroscopy techniques which are Fourier transform infrared spectroscopy (FT-IR) and nuclear magnetic resonance (NMR).

3.2.1 Fourier Transform Infrared Spectroscopy (FTIR)

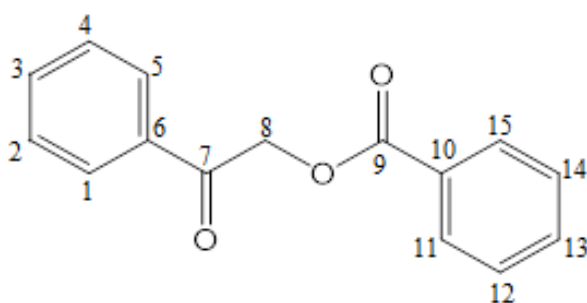
Fourier transform infrared spectroscopy (FTIR) spectra for compounds **2(a-s)** were collected on a Perkin Elmer Frontier FTIR Spectrometer 100 which is available at the School of Chemical Sciences, Universiti Sains Malaysia. The Spectrometer is equipped with attenuated total reflection (ATR) in frequency range of 4000-650 cm^{-1} (School of Chemical Sciences, USM).

3.2.2 Nuclear Magnetic Resonance (NMR)

^1H and ^{13}C nuclear magnetic resonance (NMR) spectra for compounds **2(a-s)** were obtained from a JEOL JNM-ECX 400 MHz FT-NMR Spectrometer located at the Department of Chemical Sciences, Universiti Tunku Abdul Rahman. The samples were prepared in deuterated chloroform (CDCl_3) or deuterated dimethyl sulfoxide (d_6 -DMSO) as the solvent in 5 mm NMR tubes. The chemical shifts were measured relative to the tetramethylsilane (TMS) as the internal standard.

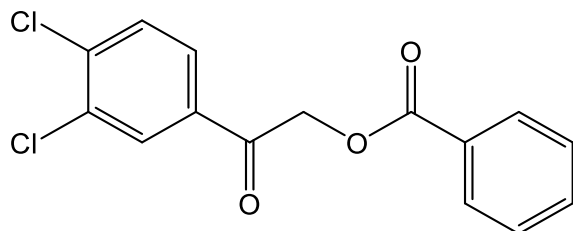
3.3 Spectroscopic Studies

The spectra data for all synthesized compounds **2(a-s)** were determined by using Fourier transform infrared (FT-IR) and nuclear magnetic resonance (NMR) spectroscopy measurements. The spectroscopic analysis were implemented using Spectrum (*Spectrum*, 2011) and Delta (*Delta*, 2014) software packages. The FT-IR and NMR results for compounds **2(a-s)** are shown as below,

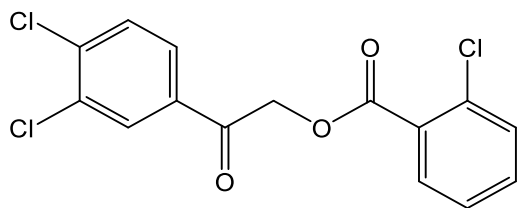


2-bromo-1-(3,4-dichlorophenyl) ethanone (1): Solvent for growing crystals: Methanol; Yield : 85% M.P.: 25-29 °C; FT-IR (ATR (solid) cm^{-1}): 3067 (Ar, C-H, ν), 3002, 2948 (C-H, ν), 1693 (C=O, ν), 1581, 1465 (Ar, C-C, ν), 1030 (C-Br, ν), 811 (C-Cl, ν); ^1H -NMR (400 MHz, CDCl_3): δ ppm 8.06 (s, 1H, 1CH), 7.82-7.78 (d, 1H, $J=8.4$ Hz, 5CH), 7.59-7.57 (d, 1H, $J=8.4$ Hz, 4CH), 4.37 (s, 2H, 8CH₂). ^{13}C -NMR (125 MHz, CDCl_3):

δ ppm 189.38 (C⁷), 138.80 (C³), 133.78 (C²), 133.50 (C⁶), 131.08 (C¹), 130.99 (C⁴), 128.04 (C⁵), 30.05 (C⁸).

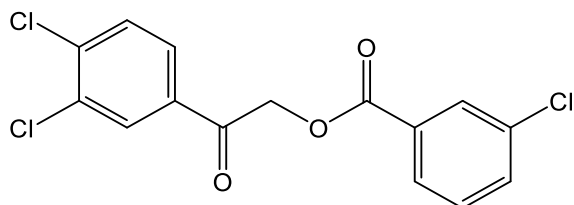


2-(3, 4-dichlorophenyl)-2-oxoethyl benzoate (**2a**): Solvent for growing crystals: Acetone; Yield : 85% M.P.: 25-29 °C; FT-IR (ATR (solid) cm⁻¹): 3062 (Ar, C-H, ν), 2945 (C-H, ν), 1717, 1701 (C=O, ν), 1600, 1417 (Ar, C-C, ν), 1289, 1216, 1134 (C-O, ν), 714 (C-Cl, ν); ¹H-NMR (400 MHz, CDCl₃): δ ppm 8.117-8.095 (d, 2H, J=8.8 Hz, 11CH, 15CH), 8.036 (s, 1H, 1CH), 7.78-7.758 (d, 1H, J=8.8 Hz, 5CH), 7.613-7.562 (m, 2H, 4CH, 13CH), 7.481-7.443 (t, 2H, J=7.6 Hz, 12CH, 14CH), 5.489 (s, 2H, 8CH₂). ¹³C-NMR (125 MHz, CDCl₃): δ ppm 190.41 (C⁷), 166.02 (C⁹), 138.68 (C³), 133.84 (C², C⁶), 133.65 (C¹³), 131.17 (C¹), 130.06 (C¹¹, C¹⁵), 129.98 (C⁴), 129.16 (C¹⁰), 128.62 (C¹², C¹⁴), 126.94 (C⁵), 66.33 (C⁸).

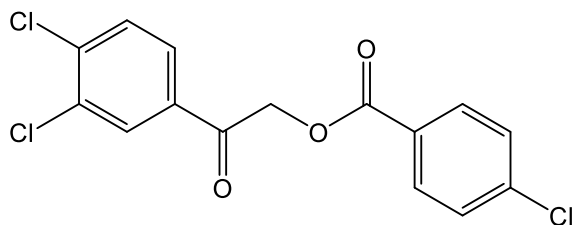


2-(3, 4-dichlorophenyl)-2-oxoethyl 2-chlorobenzoate (**2b**): Solvent for growing crystals: Acetone; Yield : 83% M.P.: 25-29 °C; FT-IR (ATR (solid) cm⁻¹): 3089 (Ar, C-H, ν), 2924 (C-H, ν), 1735, 1700 (C=O, ν), 1583, 1422 (Ar, C-C, ν), 1246, 1216, 1121, 1029 (C-O, ν), 747 (C-Cl, ν); ¹H-NMR (400 MHz, CDCl₃): δ ppm 8.048-8.006 (m, 2H, 1CH, 15CH), 7.789-7.769 (d, 1H, J=8.2 Hz, 5CH), 7.606-7.585 (d, 1H, J=8.2

Hz, 4CH), 7.496-7.441 (m, 2H, 12CH, 13CH), 7.379-7.344 (t, 1H, J=7.0 Hz, 14CH), 5.506 (s, 2H, 8CH₂). ¹³C-NMR (125 MHz, CDCl₃): δ ppm 190.40 (C⁷), 164.85 (C⁹), 138.82 (C³), 134.32 (C¹¹), 133.89 (C²), 133.72 (C⁶), 133.27 (C¹³), 132.07 (C¹⁵), 131.32 (C¹), 131.21 (C⁴), 130.00 (C⁵), 128.91 (C¹⁰), 126.91 (C¹²), 126.81 (C¹⁴), 66.48 (C⁸).

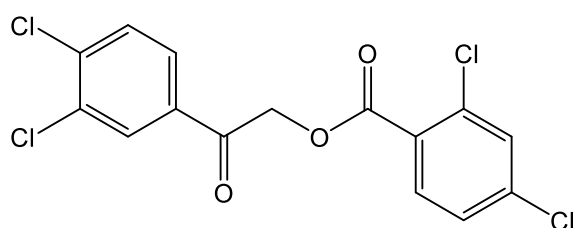


2-(3, 4-dichlorophenyl)-2-oxoethyl 3-chlorobenzoate (**2c**): Solvent for growing crystals: Acetone; Yield : 80% M.P.: 25-29 °C; FT-IR (ATR (solid) cm⁻¹): 3066 (Ar, C-H, v), 2942 (C-H, v), 1719, 1699 (C=O, v), 1575, 1466 (Ar, C-C, v), 1283, 1257, 1213, 1128 (C-O, v), 769, 744 (C-Cl, v); ¹H-NMR (400 MHz, CDCl₃): δ ppm 8.093 (s, 1H, 1CH), 8.029 (s, 1H, 11CH), 8.006-7.986 (d, 1H, J=8.2 Hz, 5CH), 7.78-7.759 (d, 1H, J=8.2 Hz, 4CH), 7.601-7.561 (m, 2H, 13CH, 15CH), 7.435-7.395 (t, 1H, J=8 Hz, 14CH), 5.505 (s, 2H, 8CH₂). ¹³C-NMR (125 MHz, CDCl₃): δ ppm 189.97 (C⁷), 164.87 (C⁹), 138.86 (C³), 134.79 (C²), 133.70 (C¹³), 133.66 (C⁶), 131.23 (C¹), 130.88 (C¹⁰), 130.13 (C⁴), 129.96 (C⁵, C¹¹), 128.20 (C¹⁴), 126.88 (C¹⁵), 66.52 (C⁸).

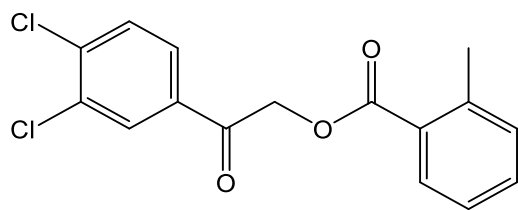


2-(3, 4-dichlorophenyl)-2-oxoethyl 4-chlorobenzoate (**2d**): Solvent for growing crystals: Acetone; Yield : 75% M.P.: 25-29 °C; FT-IR (ATR (solid) cm⁻¹): 3096 (Ar, C-H, v), 2952, 2921 (C-H, v), 1722, 1696 (C=O, v), 1586, 1433 (Ar, C-C, v), 1280,

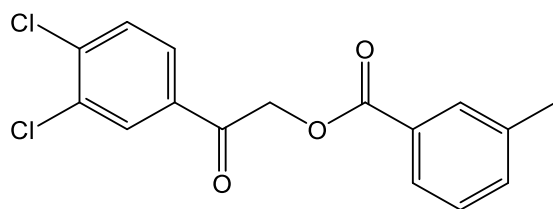
1211, 1137, 1090 (C-O, ν), 811 (C-Cl, ν); $^1\text{H-NMR}$ (400 MHz, CDCl_3): δ ppm 8.061-8.030 (m, 3H, 1CH, 11CH, 15CH), 7.786-7.764 (d, 1H, $J=8.80$ Hz, 5CH), 7.600-7.578 (d, 1H, $J=8.8$ Hz, 4CH), 7.457-7.435 (d, 2H, $J=8.8$ Hz, 12CH, 14CH), 5.490 (s, 2H, 8CH₂). $^{13}\text{C-NMR}$ (125 MHz, CDCl_3): δ ppm 190.10 (C⁷), 165.16 (C⁹), 140.18 (C¹³), 138.81 (C³), 133.88 (C²), 133.72 (C⁶), 131.45 (C¹¹, C¹⁵), 131.20 (C¹), 129.94 (C⁴), 128.99 (C¹², C¹⁴), 127.62 (C¹⁰), 126.87 (C⁵), 66.40 (C⁸).



2-(3,4-dichlorophenyl)-2-oxoethyl 2,4-dichlorobenzoate (2e): Solvent for growing crystals: Acetone; Yield : 77% M.P.: 25-29 °C; FT-IR (ATR (solid) cm^{-1}): 3058 (Ar, C-H, ν), 2942 (C-H, ν), 1730, 1702 (C=O, ν), 1581, 1421 (Ar, C-C, ν), 1247, 1215, 1102, 1029 (C-O, ν), 818 (C-Cl, ν); $^1\text{H-NMR}$ (400 MHz, CDCl_3): δ ppm 8.038-7.983 (m, 2H, 1CH, 15CH), 7.786-7.765 (d, 1H, $J=8.4$ Hz, 5CH), 7.612-7.591 (d, 1H, $J=8.4$ Hz, 4CH), 7.510 (s, 1H, 12CH), 7.357-7.337 (d, 1H, $J=8.0$ Hz, 14CH), 5.502 (s, 2H, 8CH₂). $^{13}\text{C-NMR}$ (125 MHz, CDCl_3): δ ppm 189.81 (C⁷), 163.98 (C⁹), 139.16 (C³), 138.92 (C¹³), 135.545 (C²), 133.93 (C¹¹), 133.64 (C⁶), 133.11 (C¹⁵), 131.28 (C¹), 131.24 (C⁴), 129.97 (C¹²), 127.26 (C⁵), 127.10 (C¹⁰), 126.86 (C¹⁴), 66.53 (C⁸).

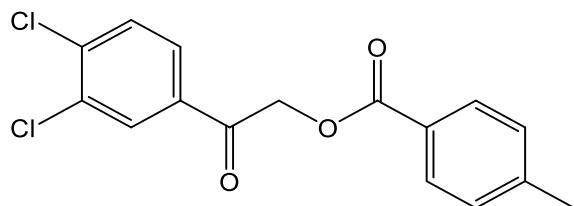


2-(3, 4-dichlorophenyl)-2-oxoethyl 2-methylbenzoate (**2f**): Solvent for growing crystals: Acetone; Yield : 80% M.P.: 25-29 °C; FT-IR (ATR (solid) cm^{-1}): 3068 (Ar, C-H, v), 2983, 2940 (C-H, v), 1722, 1702 (C=O, v), 1582, 1424 (Ar, C-C, v), 1297, 1256, 1128, 1029 (C-O, v), 738 (C-Cl, v); $^1\text{H-NMR}$ (400 MHz, CDCl_3): δ ppm 8.047-8.033 (m, 2H, 1CH, 15CH), 7.788-7.768 (d, 1H, $J=8.0$ Hz, 5CH), 7.592-7.572 (d, 1H, $J=8.0$ Hz, 4CH), 7.456-7.418 (t, 1H, $J=7.6$ Hz, 13CH), 7.292-7.252 (m, 2H, 14CH, 12CH), 5.470 (s, 2H, 8CH₂), 2.616 (s, 3H, 16CH₃). $^{13}\text{C-NMR}$ (125 MHz, CDCl_3): δ ppm 190.57 (C⁷), 166.82 (C⁹), 140.88 (C³), 138.66 (C¹¹), 133.89 (C²), 133.82 (C⁶), 132.66 (C¹³), 131.86 (C¹), 131.16 (C¹²), 131.05 (C⁴), 129.99 (C⁵), 128.53 (C¹⁰), 126.91 (C¹⁵), 125.93 (C¹⁴), 66.11 (C⁸), 21.80 (C¹⁶).

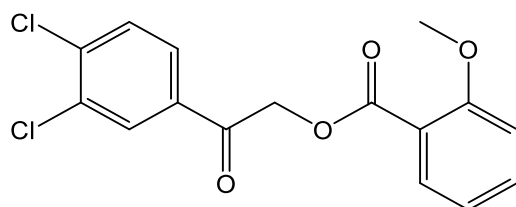


2-(3, 4-dichlorophenyl)-2-oxoethyl 3-methylbenzoate (**2g**): Solvent for growing crystals: Acetone; Yield : 85% M.P.: 25-29 °C; FT-IR (ATR (solid) cm^{-1}): 3061 (Ar, C-H, v), 2943 (C-H, v), 1701 (C=O, v), 1585, 1424 (Ar, C-C, v), 1286, 1196, 1124, 1030 (C-O, v), 753 (C-Cl, v); $^1\text{H-NMR}$ (400 MHz, CDCl_3): δ ppm 8.047 (s, 1H, 1CH), 7.927-7.903 (m, 2H, 11CH, 15CH), 7.796-7.776 (d, 1H, $J=8.0$ Hz, 5CH), 7.592-7.572 (d, 1H, $J=8.0$ Hz, 4CH), 7.418-7.333 (m, 2H, 13CH, 14CH), 5.479 (s, 2H, 8CH₂), 2.409 (s, 3H, 16CH₃). $^{13}\text{C-NMR}$ (125 MHz, CDCl_3): δ ppm 190.47 (C⁷), 166.19 (C⁹), 138.67 (C³), 138.44 (C¹²), 134.42 (C¹³), 133.90 (C²), 133.82 (C⁶), 131.16 (C¹), 130.58

(C⁴), 130.00 (C¹¹), 129.07 (C¹⁰), 128.51 (C¹⁴), 127.22 (C⁵), 126.93 (C¹⁵), 66.28 (C⁸), 21.36 (C¹⁶).

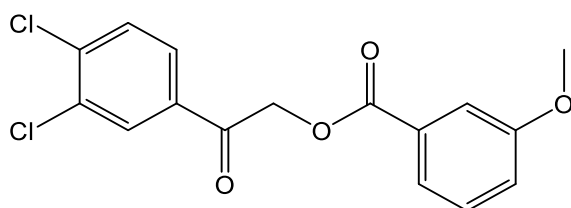


2-(3, 4-dichlorophenyl)-2-oxoethyl 4-methylbenzoate (**2h**): Solvent for growing crystals: Acetone; Yield : 83% M.P.: 25-29 °C; FT-IR (ATR (solid) cm⁻¹): 3067 (Ar, C-H, v), 2944, 2981 (C-H, v), 1708, 1698 (C=O, v), 1582, 1423 (Ar, C-C, v), 1282, 1225, 1113 (C-O, v), 757 (C-Cl, v); ¹H-NMR (400 MHz, CDCl₃): δ ppm 8.041 (s, 1H, 1CH), 8.01-7.990 (d, 2H, J=8.4 Hz, 11CH, 15CH), 7.794-7.772 (d, 1H, J=8.8 Hz, 5CH), 7.592-7.570 (d, 1H, J=8.8 Hz, 4CH), 7.275-7.253 (d, 2H, J=8.4 Hz, 12CH, 14CH), 5.466 (s, 2H, 8CH₂), 2.422 (s, 3H, 16CH₃). ¹³C-NMR (125 MHz, CDCl₃): δ ppm 190.59 (C⁷), 166.07 (C⁹), 144.46 (C¹³), 138.64 (C³), 133.92 (C²), 133.81 (C⁶), 131.15 (C¹), 130.11 (C¹¹, C¹⁵), 130.01 (C⁴), 129.33 (C¹², C¹⁴), 126.94 (C⁵), 126.40 (C¹⁰), 66.21 (C⁸), 21.84 (C¹⁶).

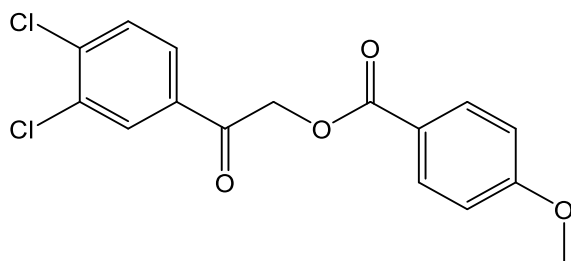


2-(3, 4-dichlorophenyl)-2-oxoethyl 2-methoxybenzoate (**2i**): Solvent for growing crystals: Acetone; Yield : 75% M.P.: 25-29 °C; FT-IR (ATR (solid) cm⁻¹): 3102 (Ar, C-H, v), 2972, 2929, 2842 (C-H, v), 1728, 1704 (C=O, v), 1581, 1463 (Ar, C-C, v), 1239, 1216, 1101, 1030 (C-O, v), 767 (C-Cl, v); ¹H-NMR (400 MHz, CDCl₃): δ ppm 8.054 (s, 1H, 1CH), 7.971-7.952 (d, 1H, J=7.7 Hz, 15CH), 7.798-7.778 (d, 1H, J=8.2

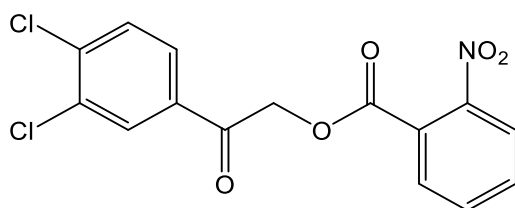
Hz, 5CH), 7.588-7.567 (d, 1H, J=8.2 Hz, 4CH), 7.535-7.496 (t, 1H, J=7.7 Hz, 13CH), 7.028-6.987 (m, 2H, 12CH, 14CH), 5.451 (s, 2H, 8CH₂), 3.907 (s, 3H, 16CH₃). ¹³C-NMR (125 MHz, CDCl₃): δ ppm 190.79 (C⁷), 165.24 (C⁹), 159.77 (C¹¹), 134.41 (C¹³), 134.03 (C²), 133.73 (C⁶), 132.34 (C¹), 131.10 (C⁴), 130.07 (C¹⁵), 127.01 (C⁵), 120.34 (C¹⁴), 118.64 (C¹⁰), 112.17 (C¹²), 66.16 (C¹⁶).



2-(3, 4-dichlorophenyl)-2-oxoethyl 3-methoxybenzoate (**2j**): Solvent for growing crystals: Acetone; Yield : 80% M.P.: 25-29 °C; FT-IR (ATR (solid) cm⁻¹): 3067 (Ar, C-H, v), 2959, 2938, 2836 (C-H, v), 1722, 1706 (C=O, v), 1582, 1453 (Ar, C-C, v), 1297, 1210, 1118, 1029 (C-O, v), 747 (C-Cl, v); ¹H-NMR (400 MHz, CDCl₃): δ ppm 8.045 (s, 1H, 1CH), 7.794-7.773 (d, 1H, J=8.4 Hz, 5CH), 7.729-7.709 (d, 1H, J=8.0 Hz, 15CH), 7.617-7.582 (m, 2H, 4CH, 11CH), 7.396-7.3556 (t, 1H, J=8.0 Hz, 14CH), 7.159-7.139 (d, 1H, J=8.0 Hz, 13CH), 5.486 (s, 2H, 8CH₂), 3.856 (s, 3H, 16CH₃). ¹³C-NMR (125 MHz, CDCl₃): δ ppm 190.35 (C⁷), 165.92 (C⁹), 159.72 (C¹²), 133.85 (C², C⁶), 131.18 (C¹), 130.40 (C¹⁰), 130.00 (C⁴), 129.66 (C¹⁴), 126.93 (C⁵), 122.51 (C¹³), 120.31 (C¹⁵), 114.33 (C¹¹), 66.38 (C⁸), 55.57 (C¹⁶).

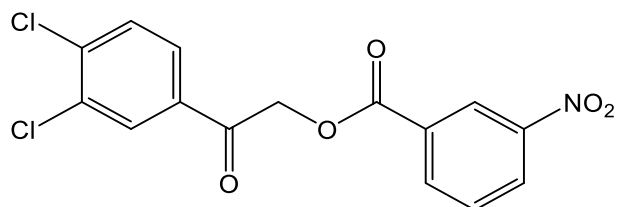


2-(3, 4-dichlorophenyl)-2-oxoethyl 4-methoxybenzoate (**2k**): Solvent for growing crystals: Acetone; Yield : 77% M.P.: 25-29 °C; FT-IR (ATR (solid) cm^{-1}): 3096 (Ar, C-H, ν), 2938, 2842 (C-H, ν), 1720, 1707 (C=O, ν), 1603, 1509 (Ar, C-C, ν), 1257, 1218, 1166, 1124 (C-O, ν), 767 (C-Cl, ν); $^1\text{H-NMR}$ (400 MHz, CDCl_3): δ ppm 8.072-8.036 (m, 3H, 1CH, 11CH, 15CH), 7.785-7.764 (d, 1H, $J=8.2$ Hz, 5CH), 7.584-7.564 (d, 1H, $J=8.2$ Hz, 4CH), 6.947-6.926 (d, 2H, $J=8.4$ Hz, 12CH, 14CH), 5.452 (s, 2H, 8CH₂), 3.865 (s, 3H, 16CH₃). $^{13}\text{C-NMR}$ (125 MHz, CDCl_3): δ ppm 190.74 (C⁷), 165.71 (C⁹), 163.94 (C¹³), 138.62 (C³), 133.92 (C²), 133.78 (C⁶), 132.18 (C¹¹, C¹⁵), 131.88 (C¹², C¹⁴), 131.14 (C¹¹), 130.00 (C⁴), 126.95 (C⁵), 121.47 (C¹⁰), 66.13 (C⁸), 55.59 (C¹⁶).

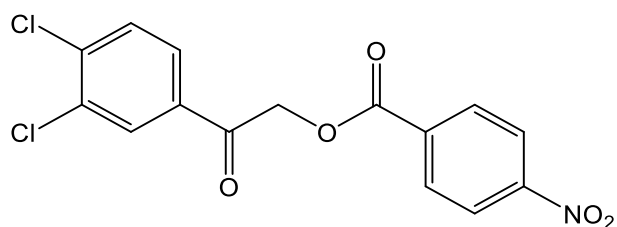


2-(3, 4-dichlorophenyl)-2-oxoethyl 2-nitrobenzoate (**2l**): Solvent for growing crystals: Acetone; Yield : 85% M.P.: 25-29 °C; FT-IR (ATR (solid) cm^{-1}): 3092(Ar, C-H, ν), 2964, 2864 (C-H, ν), 1743, 1702 (C=O, ν), 1583, 1468 (Ar, C-C, ν), 1524, 1374 (N-O, ν), 1216, 1119, 1028 (C-O, ν), 737 (C-Cl, ν); $^1\text{H-NMR}$ (400 MHz, CDCl_3): δ ppm 8.032 (s, 1H, 1CH), 8.002-7.981 (d, 1H, $J=8.2$ Hz, 15CH), 7.936-7.916 (d, 1H, $J=8.2$ Hz, 12CH), 7.780-7.725 (m, 2H, 5CH, 13CH), 7.702-7.662 (t, 1H, $J=8.2$ Hz, 14CH), 7.619-7.597 (d, 1H, $J=8.8$ Hz, 4CH), 5.518 (s, 2H, 8CH₂). $^{13}\text{C-NMR}$ (125 MHz,

CDCl₃): δ ppm 190.54 (C⁷), 165.03 (C⁹), 143.87 (C¹¹), 139.01 (C³), 133.99 (C²), 133.51 (C⁶), 133.37 (C¹³), 132.18 (C¹⁴), 131.26 (C¹), 130.37 (C⁴), 129.98 (C¹⁵), 127.09 (C¹⁰), 126.87 (C⁵), 124.18 (C¹²), 67.13 (C⁸).

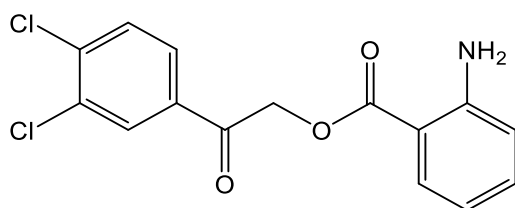


2-(3,4-dichlorophenyl)-2-oxoethyl 3-nitrobenzoate (2m): Solvent for growing crystals: Acetone; Yield : 77% M.P.: 25-29 °C; FT-IR (ATR (solid) cm⁻¹): 3072 (Ar, C-H, ν), 2952, 2869 (C-H, ν), 1730, 1702 (C=O, ν), 1585, 1441 (Ar, C-C, ν), 1525, 1348 (N-O, ν), 1259, 1138, 1028 (C-O, ν), 716 (C-Cl, ν); ¹H-NMR (400 MHz, CDCl₃): δ ppm 8.963 (s, 1H, 11CH), 8.483-8.440 (m, 2H, 13CH, 15CH), 8.042 (s, 1H, 1CH), 7.801-7.780 (d, 1H, J=8.4 Hz, 5CH), 7.722-7.682 (t, 2H, J=8.0 Hz, 14CH), 7.682-7.607 (d, 1H, J=8.4 Hz, 4CH), 5.575 (s, 2H, 8CH₂). ¹³C-NMR (125 MHz, CDCl₃): δ ppm 189.49 (C⁷), 164.01 (C⁹), 148.46 (C¹²), 139.05 (C³), 135.71 (C¹⁵), 134.01 (C²), 133.51 (C⁶), 131.29 (C¹), 131.00 (C¹⁰), 129.94 (C⁴), 129.91 (C¹⁴), 128.04 (C⁵), 126.84 (C¹³), 125.11 (C¹¹), 66.79 (C⁸).

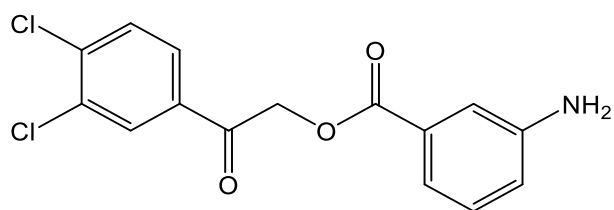


2-(3,4-dichlorophenyl)-2-oxoethyl 4-nitrobenzoate (2n): Solvent for growing crystals: Acetone; Yield : 85% M.P.: 25-29 °C; FT-IR (ATR (solid) cm⁻¹): 3081 (Ar, C-H, ν), 2937, 2860 (C-H, ν), 1728, 1703 (C=O, ν), 1606, 1416 (Ar, C-C, ν), 1523, 1346 (N-O, ν).

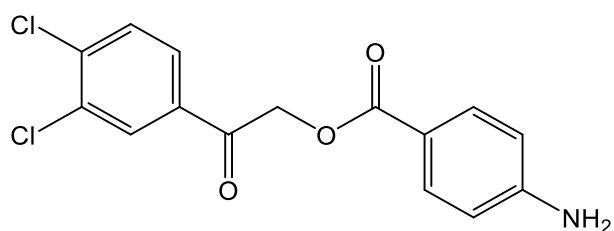
v), 1275, 1211, 1124 (C-O, v), 717 (C-Cl, v); ¹H-NMR (400 MHz, CDCl₃): δ ppm 8.343-8.285 (m, 4H, 11CH, 12CH, 14CH, 15CH), 8.037 (s, 1H, 1CH), 7.796-7.776 (d, 1H, J=8.0 Hz, 5CH), 7.624-7.604 (d, 1H, J=8.0 Hz, 4CH), 5.565 (s, 2H, 8CH₂). ¹³C-NMR (125 MHz, CDCl₃): δ ppm 189.49 (C⁷), 164.22 (C⁹), 150.97 (C¹³), 139.07 (C³), 134.58 (C²), 134.01 (C⁶), 133.51 (C¹⁰), 131.30 (C¹), 131.24 (C¹¹, C¹⁵), 129.94 (C⁴), 126.84 (C⁵), 123.77 (C¹², C¹⁴), 66.81 (C⁸).



2-(3, 4-dichlorophenyl)-2-oxoethyl 2-aminobenzoate (20): Solvent for growing crystals: Acetone; Yield : 75% M.P.: 25-29 °C; FT-IR (ATR (solid) cm⁻¹): 3478, 3361 (N-H, v), 3057 (Ar, C-H, v), 2945 (C-H, v), 1688 (C=O, v), 1611, 1455 (Ar, C-C, v), 1579 (N-H, δ), 1248, 1215, 1098, 1029 (C-O, v), 753 (C-Cl, v); ¹H-NMR 8.049 (s, 1H, 1CH), 7.977-7.957 (d, 1H, J=7.8 Hz, 15CH), 7.801-7.780 (d, 1H, J=8.4 Hz, 5CH), 7.595-7.574 (d, 1H, J=8.4 Hz, 4CH), 7.317-7.278 (t, 1H, J= 7.8 Hz, 13CH), 6.691-6.655 (m, 2H, 12CH, 14CH), 5.672 (s, 2H, NH₂), 5.435 (s, 2H, 8CH₂). ¹³C-NMR (125 MHz, CDCl₃): δ ppm 190.87 (C⁷), 167.26 (C⁹), 150.90 (C¹¹), 138.65 (C³), 134.84 (C¹³), 133.91 (C²), 133.82 (C⁶), 131.59 (C¹), 131.15 (C⁴), 130.02 (C¹⁵), 126.95 (C⁵), 116.83 (C¹²), 116.58 (C¹⁴), 109.71 (C¹⁰), 65.90 (C⁸).

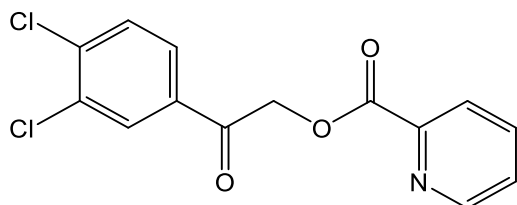


2-(3, 4-dichlorophenyl)-2-oxoethyl 3-aminobenzoate (**2p**): Solvent for growing crystals: Acetone; Yield : 77% M.P.: 25-29 °C; FT-IR (ATR (solid) cm^{-1}): 3436, 3357 (N-H, ν), 3014 (Ar, C-H, ν), 2933 (C-H, ν), 1718, 1697(C=O, ν), 1602, 1463 (Ar, C-C, ν), 1555 (N-H, δ), 1219, 1118, 1028 (C-O, ν), 740 (C-Cl, ν); $^1\text{H-NMR}$ (400 MHz, CDCl_3): δ ppm 8.045 (s, 1H, 1CH), 7.786-7.765 (d, 1H, $J=8.4$ Hz, 5CH), 7.595-7.574 (d, 1H, $J=8.4$ Hz, 4CH), 7.511-7.491 (d, 1H, $J=8.0$ Hz, 15CH), 7.406 (s, 1H, 11CH), 7.258-7.238 (t, 1H, $J=8.0$ Hz, 14CH), 6.905-6.885 (d, 1H, $J=8.0$ Hz, 13CH), 5.458 (s, 2H, 8CH₂), 3.812 (s, 2H, NH₂). $^{13}\text{C-NMR}$ (125 MHz, CDCl_3): δ ppm 190.51 (C⁷), 166.18 (C⁹), 146.66 (C¹²), 138.67 (C³), 133.89 (C²), 133.82 (C⁶), 131.16 (C¹), 130.07 (C¹⁰), 130.01 (C⁴), 129.53 (C¹⁴), 126.53 (C⁵), 120.22 (C¹³), 120.10 (C¹⁵), 116.09 (C¹¹), 66.29 (C⁸).

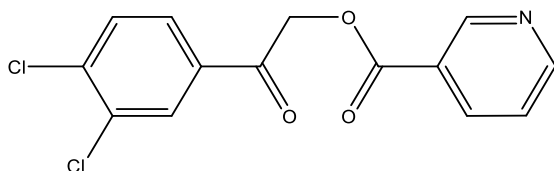


2-(3, 4-dichlorophenyl)-2-oxoethyl 4-aminobenzoate (**2q**): Solvent for growing crystals: Acetone; Yield : 80% M.P.: 25-29 °C; FT-IR (ATR (solid) cm^{-1}): 3436, 3357 (N-H, ν), 3014 (Ar, C-H, ν), 2933 (C-H, ν), 1718, 1697(C=O, ν), 1602, 1463 (Ar, C-C, ν), 1555 (N-H, δ), 1219, 1118, 1028 (C-O, ν), 740 (C-Cl, ν); $^1\text{H-NMR}$ (400 MHz, CDCl_3): δ ppm 8.047 (s, 1H, 1CH), 7.927-7.907 (d, 2H, $J=8.8$ Hz, 11CH, 15CH), 7.794-7.773 (d, 1H, $J=8.2$ Hz, 5CH), 7.585-7.565 (d, 1H, $J=8.2$ Hz, 4CH) 6.666-6.644

(d, 2H, J= 8.8 Hz, 12CH, 14CH), 5.415 (s, 2H, 8CH₂), 4.110 (s, 2H, NH₂). ¹³C-NMR (125 MHz, CDCl₃): δ ppm 191.09 (C⁷), 165.91 (C⁹), 151.44 (C¹³), 138.50 (C³), 134.10 (C²), 133.75 (C⁶), 132.23 (C¹¹, C¹⁵), 131.09 (C¹), 130.03 (C⁴), 126.96 (C⁵), 118.53 (C¹⁰), 113.93 (C¹², C¹⁴), 65.95 (C⁸).



2-(3, 4-dichlorophenyl)-2-oxoethyl picolinate (**2r**): Solvent for growing crystals: Acetone; Yield : 70% M.P.: 25-29 °C; FT-IR (ATR (solid) cm⁻¹): 3436, 3357 (N-H, v), 3014 (Ar, C-H, v), 2933 (C-H, v), 1718, 1697(C=O, v), 1602, 1463 (Ar, C-C, v), 1555 (N-H, δ), 1219, 1118, 1028 (C-O, v), 740 (C-Cl, v); ¹H-NMR (400 MHz, CDCl₃): δ ppm 8.790-8.774 (d, 1H, J=6.6 Hz, 11CH), 8.196-8.179 (d, 1H, J=6.6 Hz, 14CH), 8.032 (s, 1H, 1CH), 7.888-7.853 (t, 1H, J=6.6 Hz, 13CH), 7.786-7.765 (d, 1H, J=8.2 Hz, 5CH), 7.585-7.565 (d, 1H, J=8.2 Hz, 4CH), 7.532-7.501 (t, 1H, J=6.6 Hz, 12CH), 5.582 (s, 2H, 8CH₂). ¹³C-NMR (125 MHz, CDCl₃): δ ppm 189.64 (C⁷), 164.59 (C⁹), 150.12 (C¹¹), 147.13 (C¹⁰), 138.79 (C³), 137.27 (C¹³), 133.86 (C²), 133.64 (C⁶), 131.19 (C¹), 129.97 (C⁴), 127.54 (C¹²), 126.93 (C⁵), 125.80 (C¹⁴), 66.99 (C⁸).



2-(3, 4-dichlorophenyl)-2-oxoethyl nicotinate (**2s**): Solvent for growing crystals: Acetone; Yield : 75% M.P.: 25-29 °C; FT-IR (ATR (solid) cm⁻¹): 3436, 3357 (N-H, v), 3014 (Ar, C-H, v), 2933 (C-H, v), 1718, 1697(C=O, v), 1602, 1463 (Ar, C-C, v),